Auto-recognition Method for Pointer-type Meter Based on Binocular Vision

Biao Yang

School of Instrument Science and Engineering, Southeast University, Nanjing 210096, China
Email: yb6864171@126.com

Guoyu Lin and Weigong Zhang

School of Instrument Science and Engineering, Southeast University, Nanjing 210096, China
Email: {Andrew.lin, zhangwg}@seu.edu.cn

Abstract—**This paper presents an auto-recognition method for pointer-type meter based on computer vision. Two calibrated cameras are located in the right and left sides of the meter to capture the meter displayed images. In each displayed image, the fast Hough transform method is used to locate the approximate pointer area and then the least squares fitting method is used to determine the precise line that represents the pointer indicator. Two precise lines obtained from both right and left displayed images are reconstructed in three-dimensional space according to the epipolar constraint. The line reconstructed is then projected into the target plane to determine the true indication of the meter. Experiments show that the proposed method works very well for the dial pointer identification. The maximum uncertainty in the determination of the pointer's indication is less than the human eye can discriminate.**

Index Terms—**binocular vision, three-dimensional reconstruction, fast Hough transform, least squares fitting**

I. INTRODUCTION

The pointer-type meter is widely used in manufacturing industries for its convenience, low cost and anti-electromagnetic interference. Calibrations are needed regularly to determine whether the accuracy of the meter can meet the requirements of the industry standard. The traditional calibration method is done manually. Workers read the indications of the meters one by one to decide whether the meter is qualified according to the difference between indications and standard values. Such manual method has the drawbacks of distinct error, low efficiency and high subjectivity, etc. In order to solve the problems existing in manual calibration, an auto-recognition method for pointer-type meter based on computer aided system [1-3] and binocular vision is developed. The key issue of the method is the automatic and accurate reading of the pointer-type meter from its displayed image.

There are mainly two methods to determine the reading indication of the meter from its displayed image. One is to detect the pointer indicator and the scale it points to [4-5]. The other is to calculate the angle of the pointer indicator and then determine the reading indication according to the correspondence between the

angle and the indication. The former one is hard to execute because sometimes the scales are too obscure to identify. It is simple to read the meter according to the correspondence between the pointer angle and the indication. Thus, the key issue for auto-recognition of the pointer-type meter is to determine the angle of the pointer indicator from its displayed image. The Hough transform and the least squares fitting method are two commonly used approaches to determine the angle. The Hough transform detects the straight line which can represent the pointer indicator and then calculates the angle according to the line [6-7]. However, sometimes more than one line may be detected and it is hard to choose the most precise one from various lines. The least squares fitting method determines the straight line using the least squares fitting method [8] based on the region of the pointer indicator. However, the region is hard to well separate from the displayed image and it is easy to be influenced by noise. In this paper, both methods are combined to determine the straight line that represents the pointer indicator. The Hough transform is used to locate the approximate region of the pointer indicator and then the least squares fitting method is used to determine the precise line that represents the pointer indicator.

The reading indication of the meter may drift from the standard value even when the straight line is extracted precisely from the captured image. The angle between camera optical axis and the normal vector of meter plane may cause a distortion between the indication and the true value. This paper presents a compensation technique based on binocular vision. Fig. 1 demonstrates the whole process of the proposed auto-recognition method. Two calibrated cameras are located on both sides of the meter to capture the meter displayed images. The straight line which represents the pointer indicator is detected in each meter displayed image. Two lines from different camera views are reconstructed in three-dimensional space according to the epipolar constraint. The line in three-dimensional space is finally projected into the target plane to determine the true indication of the meter. The target plane in this paper is the plane of the calibration template which is pasted on the wall behind the meter, thus, the target plane is nearly parallel to the meter plane.
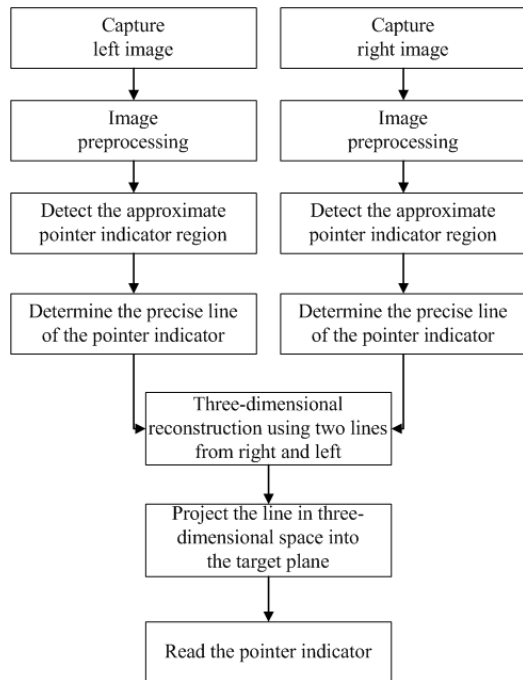
Figure 1. The flowchart of the proposed auto-recognition method.

II. CAMERA CALIBRATION

A. Figures and Tables

The camera must be calibrated to obtain its intrinsic and external parameters which will be used in three-dimensional reconstruction. Many methods have been proposed for camera calibration, such as accurate camera calibration using iterative refinement of control points [9] and linear camera calibration [10]. We will focus on the common calibration technique of Zhang Zhengyou. The method is widely used and an implementation is already available in the OPENCV library.

Zhang's method requires a calibration template with precise positioning dot matrix. Fig. 2 shows the calibration template with corners detected. Through the movement of a video camera, we can make the camera shooting template images in different locations. According to the point on the template and the homograph of its image, we can determine the intrinsic parameters of the camera, furthermore, calculate its external parameters. The model of Zhang's camera calibration method is not the main focus of this paper and we refer the reader to [11] for more details.
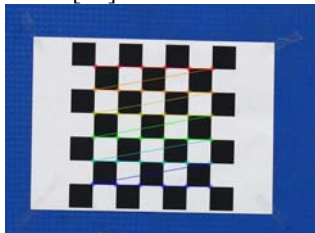
Figure 2. The calibration template with all corners detected.

III. STRAIGHT LINE EXTRACTION BASED ON MONOCULAR VISION

The key issue for accurate auto-recognition of the pointer-type meter is to extract the straight line which represents the pointer indicator in meter displayed image. This paper proposes a two-step method to extract the line. The Hough transform is used to locate the approximate region of the pointer indicator and then the least squares fitting method is used to determine the precise line that represents the pointer indicator.

A. Image Preprocessing

The auto-recognition system is designed to read more than one meter simultaneously. It is necessary to set ROI for each meter in the captured image. Each ROI is set manually due to the complex environment in where it is hard to separate the meter region from the cluttered background. After each ROI is determined, it must carry on preprocessing to facilitate following image processing, including color transformation from RGB into grayscale, noise filtering and image enhancement. Color transformation from RGB into grayscale is to reduce the computational complexity. For the noise which is inevitable in image acquisition, the median filtering can be used to reduce noise, enhance contrast and make the image smoother.

B. Image Binaryzation

After image preprocessing, the grayscale ROI image should be converted into the binary image. The fixed thresholding method cannot reach a satisfactory performance due to different meter appearances and various imaging conditions. The Ostu adaptive thresholding method [12] is employed in this paper for its effectiveness and efficiency.

The Ostu thresholding is based on the maximum variance theory. It divides all pixels of the image into two groups based on the well known probability theory that, if the inter-calss variance of the two groups is maximized, the probability of mis-dividing data of the two groups will be minimized. We have found from abundant experiments that the brightness of pointer, scales, nameplate and cover of the meter is much lower than other parts. Thus, the Ostu adaptive thresholding method can be used for image binaryzation. In the binary images as shown in Fig. 3(a), the pointer indicator is properly segmented from its displayed image. Edge is also detected based on the binary image using the canny operator, as shown in Fig. 3(b).
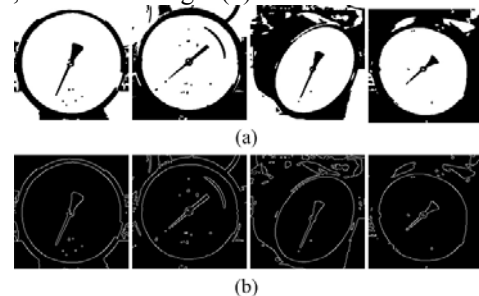
Figure 3. (a)The binary images and (b)their corresponding edge images.

C. Approximate Region of Pointer Indicator

The approximate region of the pointer indicator is located based on the straight line that represents the pointer indicator. This line can be detected by the Hough transform. A straight line can be defined by two parameters: the minimum distance (ρ) from the origin of the coordinate system (OXY) to the straight line; and the angle (θ) between the vertical axes (Y) and the straight line. Fig. 4 depicts the relationship of ρ and θ.
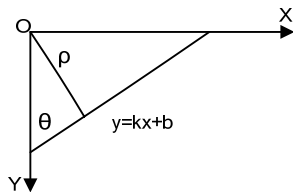
Figure 4. The relationship between $\rho\theta$ and OXY.

The Hough method transforms all points in image space (xy) into parameter space ($\rho\theta$) and then makes a statistical analysis in parameter space. The most frequent ($\rho\theta$)s are considered as potential parameters of the straight lines. The relationship between $\rho\theta$ and xy is defined as

$$\rho = x \cdot \cos(\theta) + y \cdot \sin(\theta). \qquad (1)$$

The biggest advantage of the Hough transform is the robustness of line detection even in the condition of line discontinuous caused by noise or occlusion. To improve the speed of straight line detection, a fast Hough transform based on grading [13] is employed in this paper. Compared with the traditional one, the latter is faster and more accurate.

Generally speaking, more than one straight line will be detected by the Hough transform. Thus, a weighted voting approach is proposed to determine the most possible line that represents the pointer indicator. In the voting approach, the number of detected lines in the neighborhood of one line is considered as the weight of that line. After obtaining the weight of each detected line, the line with the highest weight is considered as the potential line near which the approximate region of the pointer indicator is located. Fig. 5 shows the results of line detection using the Hough transform and the potential lines after weighted voting.
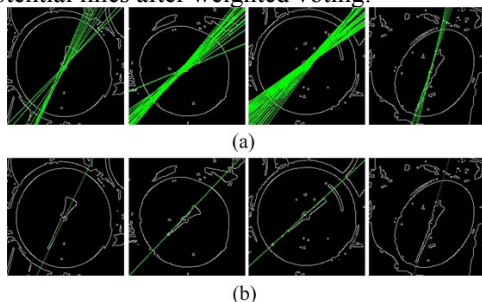
Figure 5. (a) The Hough results and (b) the potential lines after weighted voting.

D. Least Squares Fitting

The approximate region of pointer indicator is located based on the potential line obtained by the Hough transform. Then the least squares fitting method is used to determine the precise line that represents the pointer indicator in its displayed image. The least squares fitting method [14] is based on the idea that the regression fitting line for dispersed points $P(x_i, y_i)$ (i=1,2,…,n) is L: y=ax+b. The total square differences is defined as

$$f(a,b) = \text{Min} \sum_{i=1}^{n} [y_i - (ax_i + b)]^2 \qquad (2)$$

It can be seen that in (2), parameter a and b are determined by the minimum sum of the square difference of y coordinate, which means replacing two-dimensional deviation with one-dimensional deviation. To calculate the values of a and b when f(a, b) is minimum are equal to calculate the stagnation points of f(a, b). Through the derivation, the expressions of a and b can be defined as

$$a = \frac{\sum_{i=1}^{n} x_i y_i - \sum_{i=1}^{n} x_i \sum_{i=1}^{n} y_i / n}{\sum_{i=1}^{n} x_i^2 - (\sum_{i=1}^{n} x_i)^2 / n} \qquad (3)$$

$$b = \frac{\sum_{i=1}^{n} y_i - a \sum_{i=1}^{n} x_i}{n} \qquad (4)$$

The fitting precision may vary with the location of the approximate pointer indicator region and the potential noise in that region. The precision of the former one is guaranteed by accurate line extraction using the Hough transform. However, noise like characters in meter displayed image may reduce the precision of the least squares fitting.

We have found that characters like nameplates existing in the vertical direction are the main disturbance for accurate reading of the pointer indicator. Such noise can be removed by scanning the pointer region line by line. As depicted in any sub-graph of Fig. 6, the main noise such as nameplates is marked using a red rectangle which can be defined using empirical values. The pointer regions containing the pointer indicators are marked using the green rectangles which can be defined based on the binary images of the pointer indicators.
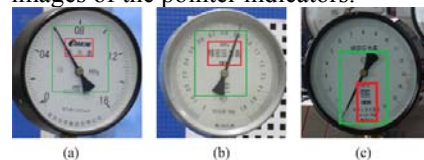
Figure 6. (a)(b)(c) Green pointer regions and red noise regions.

In general, noises such as nameplates only exist when the slopes of pointer indicators are larger than a given threshold T_1 (when the pointer indicator passes through the red rectangle). As shown in Fig. 6, the width of the pointer indicator is much smaller than the width of the pointer region. Thus, noise may exist in the line if the foreground pixel number of that line is larger than a specific threshold T_2. The flowchart of the noise removing algorithm is demonstrated in Fig. 7. The slope

of the potential line is calculated initially and then compared with T_1 to determine whether noise filtering is needed. If noise filtering is needed, the foreground pixel numbers of every line in the rectangle region are counted. If the pixel number of one line is larger than T_2, this line is discarded due to potential noise. Otherwise, the foreground pixels in that line can be added into the fitting points set. Thresholds T_1 and T_2 are determined by experiments.
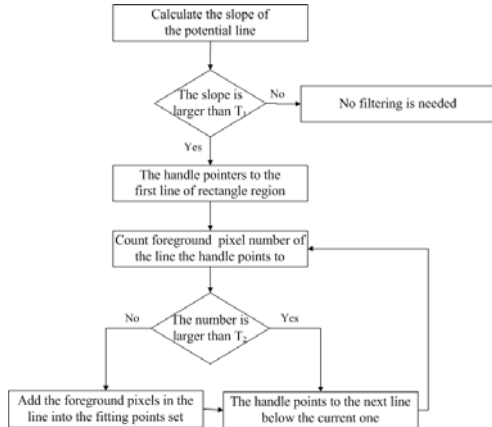
Figure 7. The flowchart of the proposed noise filtering method.

The direction of the pointer is needed to determine the precise line. Generally speaking, the head of the pointer is more tenuous than its tail. The average distance between pixels in pointer's head and the center of ROI is larger than that between pixels in pointer's tail and the center of ROI. Fig. 8 (a)(c) shows the discriminative ability of the proposed method to distinguish pointer's head from its tail. The red region indicates the pointer's head while the green one indicates its tail. The fitting results of the lines after noise filtering are given in Fig. 8(b)(d).

| (a) | (b) | (c) | (d) |
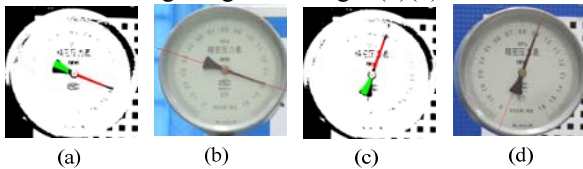
Figure 8. (a),(c) The discriminative ability of the proposed method to distinguish pointer's head from its tail. (b),(d) Fitting results of the lines that represent the pointer indicators.

IV. THREE-DIMENSIONAL RECONSTRUCTION

Errors always exist in reading the meter based on monocular vision even when the line representing the pointer indicator is precisely detected. The angle between camera optical axis and the normal vector of meter plane may cause a distortion between the indication and the true value. A compensation technique based on binocular vision is proposed in this paper. The three-dimensional coordinates of the pointer indicator is calculated and then projected into the target plane. The true line that represents the pointer indicator is calculated using the least squares fitting based on the projected points in the target plane.

A. Matching Points Extraction

A geometric constraint relationship exists on the same objects' images under the same world coordinate system. In stereo vision, we can use image points matching to recover this relationship, on the contrary, use the relationship to restrict the candidate matching points, which transforms the scope of the searching for the corresponding points from the two-dimensional plane to a one-dimensional line.
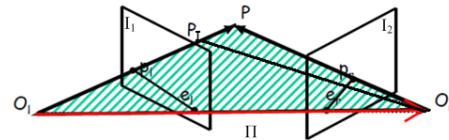
Figure 9. Principle of the epipolar constraint.

Fig. 9 demonstrates the principle of the epipolar constraint [15-16]. As shown in the figure, P_l and P_r are two projection points of the same space point P. Straight line $P_l e_l$ is the epipolar line corresponding to P_r and straight line $P_r e_r$ is the epipolar line corresponding to P_l. Assuming a point P_l whose projection in left image I_1 is P_l, the matching point in right image I_2 is inevitably on the epipolar line $P_r e_r$ which is corresponding to P_l. Thus, given two lines in the left image and the right image respectively, the method to extract matching points based on the epipolar constraint is defined as follows.

1) Sample a point X_{1i} (i=1 initially) on the straight line of the left image as an interest point.

2) Calculate the epipolar line corresponding to X_{1i}. The intersection of the epipolar line and the straight line of the right image is considered as the candidate matching point X_{2i}.

3) Take X_{2i} in the right image as the interest point and repeat the process of step 2) to find the candidate point X_{3i} in the left image which matches with X_{2i}.

4) If X_{1i} equal to X_{3i}, X_{1i} and X_{2i} matches successfully, otherwise the point X_{1i} will be discarded. Sample a point $X_{1(i+1)}$ (i=i+1 if the point can be sampled) next to X_{1i} on the straight line of the left image and go to step 2). The algorithm will be terminated if no appropriate point can be sampled.

B. Three-dimensional Reconstruction

Three-dimensional reconstruction [17-18] is used to calculate the coordinates of the pointer indicator in world coordinate. It is implemented based on the matching points obtained according to the epipolar constraint. A three-dimensional reconstruction method with calibrated cameras [19] is employed in this paper. The fundamental matrix is estimated initially based on the intrinsic and extrinsic parameters of two cameras. Then, the rotation and translation of the right camera relative to the left one are calculated and the projection matrix is obtained. Finally, the three-dimensional spatial coordinates of the pointer indicator are calculated using triangulation measurement based on information obtained before. Fig. 10 depicts the results of the three-dimensional reconstruction. The depth information of the pointer indicator is revealed by the Z coordinate. As shown in the

figure, meters (a) and (b) are almost stable in Z axis with tiny variation (about 5mm). Meter (c) is unstable in Z axis with a variation of 25mm. The stabilities of Z axis indicate that meters (a) and (b) are almost parallel to the target plane while the meter (c) is slightly inclined. Final reading indications of meters (a) and (b) are more accurate than those of meter (c) due to their stabilities in Z axis.
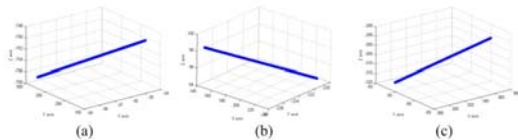
Figure 10. Results of three-dimensional reconstruction of meters (a), (b) and (c).

The three-dimensional coordinates of the pointer indicator are projected into the target plane. The straight line which reflects the actual condition of the pointer indicator is calculated using the least square fitting method based on the two-dimensional projected points. Then, the angle of the pointer indicator can be calculated using the slope of the straight line.

V. CALCULATION OF READING INDICATION

The reading indication of the meter is calculated based on the angle of the pointer indicator θ and scale information of the meter. The relationship between the reading indication v and the angle θ is defined as

$$v = n\ \frac{\theta_{up} - \theta}{\theta_{up} - \theta_{low}} \qquad (5)$$

where θ_{low} indicates the angle of the starting measuring range, θ_{up} indicates the angle of the maximal measuring range, n indicates the number of all scales.

VI. EXPERIMENTAL RESULTS

An auto-recognition system for pointer-type meter based on computer vision is built with the help of OPENCV library. Fig. 11 shows the user interface of the system. The control panel in the right part of Fig. 11 can realize the functions such as image reading, addition or deletion of ROIs. The image and ROIs are displayed in the left part of the user interface.

Figure 11. System user interface.

Fig. 12 demonstrates the results of different line extraction approaches. Fig. 12(a),(c) show the results of line extraction using the Hough transform only. Fig. 12(b),(d) show the result of line extraction using our method. As shown in the figure, lines extracted using the

Hough transform maybe drift from their real positions while lines extracted using our method are more precise. As a result, the final reading indications using our method are more accurate than the reading indications based on the lines detected by the Hough transform only.
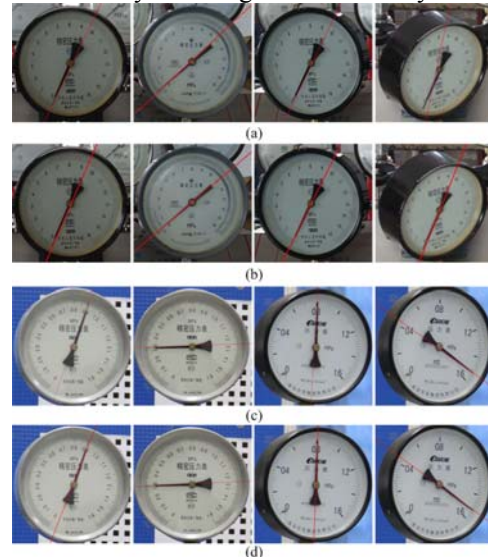
Figure 12.(a),(c) Line extraction using the Hough transform only and (b),(d) line extraction using our method.

Fig. 13 demonstrates the results of line extraction based on the meter displayed images captured by both cameras and the extractions of matching points. (a), (c) are images captured by the left camera and (b), (d) are those captured by the right camera. In the meter displayed image, the red line represents the pointer indicator and the green points on the red line represent the matching points which are extracted according to the epipolar constraint. As shown in the figure, both the lines and the matching points are extracted with a high precision.

Table Ⅰ shows the reading results of the meter displayed images using the proposed method. To demonstrate the superiority of our method, the reading results based on monocular camera are also calculated. From table 1 we can see that the reading results using our method are more accurate than reading results based on monocular camera. Precision advance P_a is calculated as follows.

$$P_a = \frac{\min(|T_L - T_S|, |T_R - T_S|) - |T - T_S|}{H} \qquad (6)$$
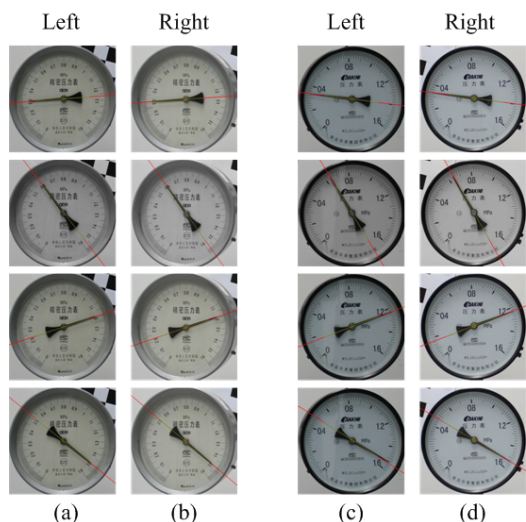
Figure 13. (a),(c) Extractions of straight lines and matching points in the left captured image and (b),(d) Extractions of straight lines and matching points in the right captured image.

where T_L and T_R are reading results of the left camera and the right camera, respectively. T is the reading result using our method and T_S is the standard value. H represents the maximum measurement range of the meter.

TABLE I.

READING RESULTS OF DIFFERENT METERS.

Results of left camera	Results of right camera	Results using our method	The standard value	Precision advance
0.1412	0.1432	0.1518	0.15	0.3125%
0.2906	0.2936	0.3029	0.3	0.2188%
0.4858	0.4902	0.5038	0.5	0.375%
0.6912	0.7042	0.7025	0.7	0.1063%
0.7912	0.7956	0.8032	0.8	0.075%
0.8923	0.8957	0.9012	0.9	0.1938%
1.2921	1.3049	1.3008	1.3	0.2563%
1.4932	1.5063	1.5011	1.5	0.325%

VII. CONCLUSION

This paper proposes a new auto-recognition method for pointer-type meter. Binocular vision is used in this paper to rectify the distortion existing in monocular vision. A two-step line extraction method is proposed to calculate the straight line that represents the pointer indicator in single camera view. The Hough transform is used to locate the approximate region of the pointer indicator and the least square fitting method is used to calculate the precise line. Experimental results validate the feasibility and accuracy of the proposed method. However, the computational complexity of the method is a little large and it is necessary to improve the speed of the method with satisfied accuracy.

ACKNOWLEDGMENT

REFERENCES

[1] Y. H. Xia, Z. Y. Wang, and W. Wang, "Blind measurement of blocking artifacts of images based on edge and flat-region detection," *Journal of Software*, vol.8, no.1, pp.168-175, 2013.

[2] C. F. Yang, F. L. Liu, and Y. Zeng, "Fusion of two typical quantitative steganalysis based on svt," *Journal of Software*, vol.8, no.3, pp.731-736, 2013.

[3] C. Y. Tsai, A. H. Tsao, and C. W. Wang, "Real-time feature descriptor matching via a multi-resolution exhaustive search method," *Journal of Software*, vol.8, no.9, pp.2197-2201, 2013.

[4] Y. Q. Yang, Y. Q. Zhao, and X. Y. He, "Automatic Calibration of Analog Measuring Instruments Using Computer Vision," *Chinese Journal of Scientific Instrument*, vol. 22, no.3, pp. 233–235, 2001.

[5] L. S. Zhang, C. H. Sui, and J. P. Tong, "Automatic recognition of analog pointer meter based on image processing method," *Journal of Zhe Jiang University of Technology*, vol.36, no.3, pp. 242-245, 2008.

[6] F. C. Alegria and A. C. Serra, "Automatic Calibration of Analog and Digital Measuring Instruments Using Computer Vision," *IEEE Transl. Instru. Meas*, vol.49, no.1, pp.94-99, 2000.

[7] Y. Wei and Y. Q. Yang, "Automatic detection equipment for index-instrument," *Electrical Measurement and Instrumentation*, vol.41, no.10, pp.30-34, 2004.

[8] W. Ye, J. D. Hu and W. B. Zou, "An auto-recognition system for pointer-meter based on TLS analytic resolution," *Proceedings of the 2009 International Conference on Networking and Digital Society*, Gui Yang, Gui Zhou, pp.83-86, 2009.

[9] A. Datta, J. S. Kim, and T. Kanade, "Accurate Camera Calibration using Iterative Refinement of Control Points," *Proceedings of the 12th International Conference on Computer Vision Workshops*, Kyoto, Japan, pp.1201-1208, 2010.

[10] X. G. Lu, Y. Wang and D. W. Yang, "Research on the Camera Linear Calibration Approach Based on the Computer Vision," *Transactions of Shen Yang Li Gong University*, vol.26, no.5, pp.43-46, 2007.

[11] Z. Y. Zhang, "A flexible new technique for camera calibration," *IEEE Trans. Pattern Analysis. Machine Intelligent*, vol.22, no.11, pp.1330-1334, 2000.

[12] M. Li and J. H. Yan, "Improvement on Canny operator by algorithm of self-adaptive determining double-threshold," *Journal of Jilin University (Engineering and Technology Edition)*, vol.38, no.4, pp.913-918, 2008.

[13] L. Yi, "Fast Hough Transform Straight Line Detection Based on Classification," *Microcomputer Information*, vol.23, no.11, pp.206-208, 2007.

[14] Y. C. Liu and F. Zhu, "Relation between Line Fitting Error and Direction of the Line in Binary Image," *Pattern Recognition and Artificial Intelligence*, vol.19, no.5, pp. 680-684, 2006.

[15] G. Y. Lin, W. G. Zhang and X. Chen, "High Precision Measurement Method of Parameters of Plane Circle Based on Stereo Vision," *Application Research of Computer*, vol.27, no.3, pp. 1183-1186, 2010.

[16] H. Peng and Y. H. Wen, "Stereo Matching for Binocular Citrus Images using Surf Operator and Epipolar Constraint," *Proceedings of the 2010 2nd International Conference on Information Engineering and Computer Science*, Wuhan, China, pp.1-4, 2010.

[17] M. L. Hu and D. Liang, "A Fast Algorithm of Hierarchical Reconstruction," *Journal of System Simulation*, vol.13 (suppl.), pp.155-158, 2010.
[18] Z. Feng and Z. R. Jiang, "A New Algorithm for Three-dimensional Construction Based on the Robot Binocular Stereo Vision System," *Proceedings of the 2012 4th International Conference on Intelligent Human-Machine Systems and Cybernetics*, Nanchang, Jiangxi, pp.302-305, 2012.
[19] C. Tomasi and T. Kanade, "Shape and motion from image streams under orthography: a factorization method," *International Journal of Computer Vision*, vol.9, no.2, pp.137-154, 1992.

Biao Yang was born in Changzhou, China in 1987. He received the B.S. degree in Nanjing University of Technology, Nanjing, China, in 2008. Currently, he is a PhD candidate in Instrument Science & Engineer of Southeast University, Nanjing, China. His research interests include pattern recognition, embedded system and computer vision with emphasis on target tracking.

Guoyu Lin was born in Fuzhou, China in 1979. He received his M.S., B.S. and PhD degrees in Nanjing University of Technology, Nanjing, China, in 2008. He is now an associate professor in Southeast University. His research interests include indoor robot navigation, lane departure warning and target tracking.

Weigong Zhang was born in Hangzhou, China in 1959. He received the M.S and B.S. degrees in Nanjing University of Aeronautics and Astronautics, Nanjing, China. He is now a professor in Instrument Science & Engineer of Southeast University, Nanjing, China. His research interests include vehicle measurement and control, sensor technology and signal processing.